*J Toxicol Pathol 2022; 35: 333–343*

**Original Article**

# Kidney organoid derived from renal tissue stem cells is a useful tool for histopathological assessment of nephrotoxicity in a cisplatin-induced acute renal tubular injury model

Shota Ueno[1,2*†], Kenji Kokura[3], Yasushi Kuromi[4], Mitsuhiko Osaki[1,5], Futoshi Okada[1,5], Shinji Kitamura[6], and Tetsuya Ohbayashi[4]

[1]Division of Experimental Pathology, Department of Biomedical Sciences, Faculty of Medicine, Tottori University, 86 Nishi-cho, Yonago, Tottori 683-8503, Japan
[2]Research and Development Division, Kikkoman Corporation, 338 Noda, Noda, Chiba 278-0037, Japan
[3]Department of Biomolecular Science, Faculty of Science, Toho University, 2-2-1 Miyama, Funabashi, Chiba 274-8510, Japan
[4]Animal Research Facility, Advanced Medicine & Translational Research Center, Organization for Research Initiative and Promotion, Tottori University, 86 Nishi-cho, Yonago, Tottori 683-8503, Japan
[5]Chromosome Engineering Research Center, Tottori University, 86 Nishi-cho, Yonago, Tottori 683-8503, Japan
[6]Department of Nephrology, Rheumatology, Endocrinology and Metabolism, Okayama University Graduate School of Medicine, Dentistry and Pharmaceutical Sciences, 2-5-1 Shikata-cho, Okayama 700-8558, Japan

**Abstract:** Organoids derived from renal tissue stem cells (KS cells) isolated from the S3 segment of adult rat nephrons have previously been developed and evaluated. However, data regarding the histopathological evaluation of these organoids are limited. Therefore, in this study, we performed histopathological examinations of the properties of these organoids and evaluated the nephrotoxicity changes induced by cisplatin treatment. We observe that the tubular structure of the organoids was generally lined by a single layer of cells, in concordance with previous findings. Microvilli were exclusively observed under electron microscopy on the luminal side of this tubular structure. Moreover, the luminal side of the tubular structure was positive for aquaporin-1 (Aqp1), a marker of the proximal renal tubule. Cisplatin treatment induced cell death and degeneration, including cytoplasmic vacuolation, in cells within the tubular structure of the organoids. Cisplatin toxicity is associated with the induction of γ-H2AX (a marker of DNA damage) and the drop of phospho-histone H3 (a marker of cell division) levels. During the nephrotoxicity assessment, the kidney organoids displayed various features similar to those of the natural kidney, suggesting that it is possible to use these organoids in predicting nephrotoxicity. The histological evaluation of the organoids in this study provides insights into the mechanisms underlying nephrotoxicity. (DOI: 10.1293/tox.2022-0006; J Toxicol Pathol 2022; 35: 333–343)

**Key words:** organoids, kidney, cisplatin, immunohistochemistry

## Introduction

*In vitro* assay systems capable of evaluating organ-specific toxicity are warranted. Although previous *in vitro* studies have made use of conventional culture methods such as monolayers on plates or suspensions in different media, the 3D-structure culture called organoids, which consist of multiple types of cells—including stem cells—capable of imitating organ-specific tissues, have recently been developed[1–4]. Compared with conventional culture methods, the characteristics of 3D organoids resemble those of the tissue in the living body more closely. Therefore, 3D organoids can be used more accurately to perform toxicity tests[5, 6].

Though several studies have reported the development of organoids mimicking various tissues[1–8], kidney organoids derived from cell lines (KS cells) isolated from the S3 segment of adult rat renal proximal tubules, by Kitamura *et al*., are quite unique as they have the nephron-like-structure[9, 10]. This organoid is characterized by an outward extension of the tubular structure into the extracellular matrix gel, Matrigel. Various analyses of these organoids have been conducted, including fluorescent immunohistochemistry of renal markers in isolated tubular structures, polymerase chain reaction (PCR) analysis of gene expression, and electron microscopy[9]. In addition, the induction of cell death follow-

Received: 14 January 2022, Accepted: 23 June 2022
Published online in J-STAGE: 18 July 2022
*Corresponding author: S Ueno
(e-mail: sueno@mail.kikkoman.co.jp)
†Present address: Research and Development Division, Kikkoman Corporation, 338 Noda, Noda, Chiba 278-0037, Japan

ing exposure to cisplatin was confirmed by Kuromi *et al*. using uptake tests of propidium iodide (PI) (manuscript in preparation). However, to further elucidate the properties of these organoids, additional detailed analyses including morphological evaluations are warranted.

As reported by Fujii *et al*., recently, many scientists are beginning to use histopathological methods to analyse organoids[4]. Detailed morphological observations of cells derived from organoids will provide insights into the molecular mechanisms underlying toxicity, thereby allowing for more accurate prediction of drug toxicity. Therefore, this study aimed at investigating the histopathological characteristics and mRNA expression patterns of this newly developed kidney organoid and analysing the toxic effect of cisplatin-induced renal tubular injury.

## Materials and Methods

### *Cell culture and differentiation*

The cell line and culture methods used in this study have been previously described by Kitamura *et al*[9]. In a brief note, KS cells which were transferred from Kitamura *et al*. were cultured on a type IV collagen plate (Corning Life Sciences, Kennebunk, ME, USA) and maintained in a 1:1 mixture with a conditioned culture supernatant (DMEM [Thermo Fisher Scientific, Waltham, MA, USA] containing 10% fetal calf serum [Thermo Fisher Scientific]) from mouse mesenchymal cells and modified K1 medium at 37°C with 5% $CO_2$/ 100% humidity. The modified K1 medium comprised of a 1:1 mixture of Dulbecco's Modified Eagle's Medium (DMEM) and Ham's F-12 medium (Thermo Fisher Scientific), supplemented with 10% FCS, 5 μg/mL insulin, 2.75 μg/mL transferrin, 3.35 ng/mL sodium selenious acid (Thermo Fisher Scientific), 50 nM hydrocortisone (Sigma, St. Louis, MO, USA), 25 ng/mL hepatocyte growth factor (Sigma), and 2.5 mM nicotinamide (Sigma).

KS cell sheets were incubated with trypsin (Thermo Fisher Scientific) and harvested. Cell clusters were obtained from the KS cells using the "hanging drop" method and these were incubated at 37°C and 5% $CO_2$/ 100% humidity for approximately 6 h. Each cluster contained approximately $1.0 \times 10^5$ KS cells. Cell clusters were then transferred into a "half Matrigel" solution situated on the filters of transwell inserts in wells containing the differentiation medium. The "half Matrigel" solution comprised a 1:1 mixture of Matrigel (Corning Life Sciences) and differentiation medium. The differentiation medium contained DMEM/ F-12 supplemented with 10% FCS, 250 ng/mL glial cell line-derived neurotrophic factor (GDNF) (R&D Systems, Minneapolis, MN, USA), 250 ng/mL basic fibroblast growth factor (bFGF) (R&D Systems), 250 ng/mL epidermal growth factor (EGF) (R&D Systems), 250 ng/mL bone morphogenetic protein-7 (BMP-7) (R&D Systems), and 250 ng/mL hepatocyte growth factor (HGF) (Sigma). Cell clusters in the "half Matrigel" solution were then cultured for up to 20 days to yield organoids.

### *Toxicity analysis of cisplatin*

Regarding the toxicity analyses, organoids cultured in the "half Matrigel" solution for 14 days were placed in different differentiation media each supplemented with 0, 20, or 30 μM cisplatin (FUJIFILM Wako Pure Chemical Corporation, Osaka, Japan) for 24, 48, or 144 h and with 10 μM cisplatin for 24 and 144 h. Exposure to cisplatin at 0, 10, and 20 μM for 144 h was performed several times (n=3 or 4). Exposure to all the other conditions was performed once, with n=2. To serve as controls, organoids cultured without cisplatin for the same duration were prepared.

### *Histological analysis*

After exposure to cisplatin, the organoids were fixed in 4% paraformaldehyde (FUJIFILM Wako Pure Chemical Corporation) at room temperature for 30 min, washed with phosphate-buffered saline (PBS), and subsequently embedded into a paraffin wax using routine procedures. Paraffin-embedded samples were 4 μm thick and were stained with haematoxylin and eosin (HE) for morphological examination. Also, immunohistochemical analysis and Terminal deoxynucleotidyl transferase dUTP nick-end labeling (TUNEL) assays were conducted on the samples to further examine their characteristics. The severity of the cytotoxicity was evaluated and scored for the different HE sections of the organoids of each group with different cisplatin exposure doses and durations. The scoring criteria were as follows: − = no dead cells in the tubular structure; + = a few dead cells in the tubular structure (less than 10% of all cells in the tubule); ++ = many dead cells in the tubular structure (approximately 10 to 50% of all cells in the tubule). +++ = over 50% of all cells in the tubular structure were dead.

### *Immunohistochemical analysis*

Immunohistochemical analyses were performed on the sections to confirm the nature of the cells constituting the organoids[11–14]. Endogenous peroxidase was blocked by treating the sample with 3% hydrogen peroxide in methanol for 12 min. For antigens retrieval, sections were treated with a citrate buffer (pH 6.0) (Agilent, Santa Clara, CA, USA) by heating in a microwave (95°C) for 30 min. After incubation with each primary antibody at 4°C overnight, immunolabeled antigens were visualized using the Simple stain rat Max-PO (Nichirei Bioscience, Tokyo, Japan) and Simple Stain DAB solution (Nichirei Bioscience), and the sections were subsequently counterstained with haematoxylin.

Several primary antibodies were used in this study. A polyclonal rabbit anti-aquaporin-1 (Aqp1) antibody (#2219, 1:2,000, Millipore, Bedford, MA, USA) was used as a marker for the renal proximal tubule. A polyclonal rabbit anti-phospho-histone H2A.X (Ser139) antibody (γ-H2AX, #2577, 1:200, Cell Signaling Technology, Danvers, MA, USA) was used for the detection of DNA damage (this antibody was used in the analysis of organoids treated with cisplatin at concentrations of 30 μM for 24 h and 10 μM for 144 h). A monoclonal rabbit anti-Ki-67 antibody (ab16667, 1:100, Abcam, Cambridge, UK) was used for the detection

of cell proliferation; this antibody was used in the analysis of organoids with cisplatin at concentration of 10 and 20 μM for 144 h. A polyclonal rabbit anti-phospho-histone H3 (Ser10) antibody (#9701, 1:200, Cell Signaling Technology) was used for the detection of cell division; this antibody was used in the analysis of organoids with cisplatin at a concentration of 30 μM for 144 h. A polyclonal rabbit anti-cleaved caspase 3 (Asp175) antibody (#9661, 1:300, Cell Signaling Technology) was used to detect apoptosis; this antibody was used to analyse organoids treated with cisplatin at a concentration of 20 μM for 144 h. For phospho-Histone H3 and Ki-67, the proportion of positive cells was counted using sections of organoids subjected to 20 μM cisplatin for 144 h (n=4 for both). Three tissue sections of each organoid at different levels were prepared, and five randomly selected fields, including the tubular structure, were imaged using a 20 × objective lens for each section. All cells in the images, including positive cells, were counted, and the proportion of positive cells was determined.

### *Transferase dUTP nick end labeling (TUNEL) assay*

Terminal deoxynucleotidyl TUNEL assay was performed using a commercially available kit from Trevigen (Gaithersburg, MD, USA) following the manufacturer's protocol. Briefly, deparaffinized and rehydrated tissue sections were washed with PBS, incubated with proteinase K (15 min), washed, and quenched before labeling with biotin-labelled dUTP. The labelling reaction was subsequently stopped by adding a stop buffer, as provided. The tissue sections were then incubated with HRP-conjugated streptavidin for 10 min, washed, and immersed in 3,3′-Diaminobenzidine (DAB) solution for colour development. The sections were counterstained with haematoxylin. The TUNEL assay was performed for the analysis of organoids with cisplatin at a concentration of 10 μM for 144 h.

### *Electron microscopy*

For electron microscopic examinations, whole organoids were immersed overnight in 0.1 M cacodylate buffer containing 2.5% glutaraldehyde (pH 7.2) and 2% paraformaldehyde. They were then dehydrated using ascending grades of ethanol, embedded in Epon, and finally cut into cubes with 2 mm sides. Ultrathin sections were stained with uranyl acetate and lead citrate and examined using a JEM-1400 transmission electron microscope (Japan Electron Optics Laboratory Co., LTD, Tokyo, Japan) at 80 kV.

### *RNA isolation and quantitative real-time PCR for the evaluation of mRNA expression*

Ten organoids cultured for 14 days were prepared and mixed to form a single sample. Two-dimensional (2D) cultured KS cells on a 10-cm plate dish at approximately 70% confluency were also collected as controls. Total RNAs were extracted from whole samples using an RNeasy mini prep kit (Qiagen, Hilden, Germany) according to the manufacturer's instructions. The total RNA concentration and quality were determined using a spectrophotometer (ND2000; Thermo Fisher Scientific). Complementary DNA (cDNA) was synthesized from the total RNA using a reverse transcription polymerase chain reaction (RT-PCR) kit (TaKaRa, Shiga, Japan), according to the manufacturer's instructions.

Gene expression was analysed via quantitative polymerase chain reaction (qPCR) using primers specific for Aqp1, Mate1, megalin, OCT1 (*Slc12a1*), and OCT2 (*Slc12a2*), which are representative proximal tubular markers and transporters. Hprt1 was selected as an internal control. For Aqp1, OCT1, and Hprt1, we obtained previously validated primer sequences from earlier studies[15–17]. For Mate1, megalin, and OCT2, primer sequences were designed using the Basic Local Alignment Search Tool, National Center for Biotechnology Information (BLAST, NCBI) to confirm the specificity of each primer pair. qPCR was performed using THUNDERBIRD® SYBR® qPCR Mix (TOYOBO, Osaka, Japan), according to the manufacturer's instructions. The reactions were performed in triplicates for each sample using a StepOnePlus Real-Time PCR System (Thermo Fisher Scientific). The cycling conditions were as follows: 95°C for 2 min; 41 cycles of 95 °C for 15 s, 60°C for 1 min, and 95°C for 15 s. Since amplification efficiency was maintained for each primer set, the expression level of each target gene was assessed using the $2^{-\Delta Ct}$ equation. The expression levels of each target gene were calculated relative to the Hprt1 levels. Gene expression data were presented as fold-change values in 3D cultures relative to those in 2D cultures.

The sequences of the primer sets used in this study were as follows: Aqp1 *fwd*-5ATT GCA GCG TCA TGT CTG AG, *rev*-5GAA CTA GGG GCA TCC AAA C; Mate1 *fwd*-5TCG TGG GCT ACA TTT TCA CCA, *rev*-5CAC CAC AGG TAC AGG CAA GA; Megalin *fwd*-5GTT CCA TTG TGG TGC ATC CG, *rev*-5GGT GAG AAC CAT CGC TCC AT; OCT1 *fwd*-5TGG CCG TAA GCT CTG TCT CT, *rev*-5TCA AGG TAT AGC CGG ACA CC; OCT2 *fwd*-5TGT GCT GTT GCT ACC TGA GA, *rev*-5CGG TCT GCT TGC TTG ACT TG; Hprt1 *fwd*-5GCG AAA GTG GAA AAG CCA AGT, *rev*-5GCC ACA TCA ACA GGA CTC TTG TA.

### *Statistical analyses*

Significant differences in gene expression, proportion of phospho-histone H3-positive cells, and Ki-67-positive cells were analysed using Student's t-test. Statistical significance was set at $p<0.05$.

## Results

### *Histology of organoids derived from KS cells*

KS cells were cultured in accordance with the procedures established by Kitamura *et al*., and the organoids obtained demonstrated a tubular structure radially extending from the center of the cluster, as previously reported[9]. After 20 days of 3D culture, single organoids approached the edge of the 24-well Transwell inserts (Fig. 1A). Paraffin sections were prepared from these organoids and HE-stained sections were subsequently examined (Fig. 1B). At the site of the tubular structure in the organoids, there was approxi-

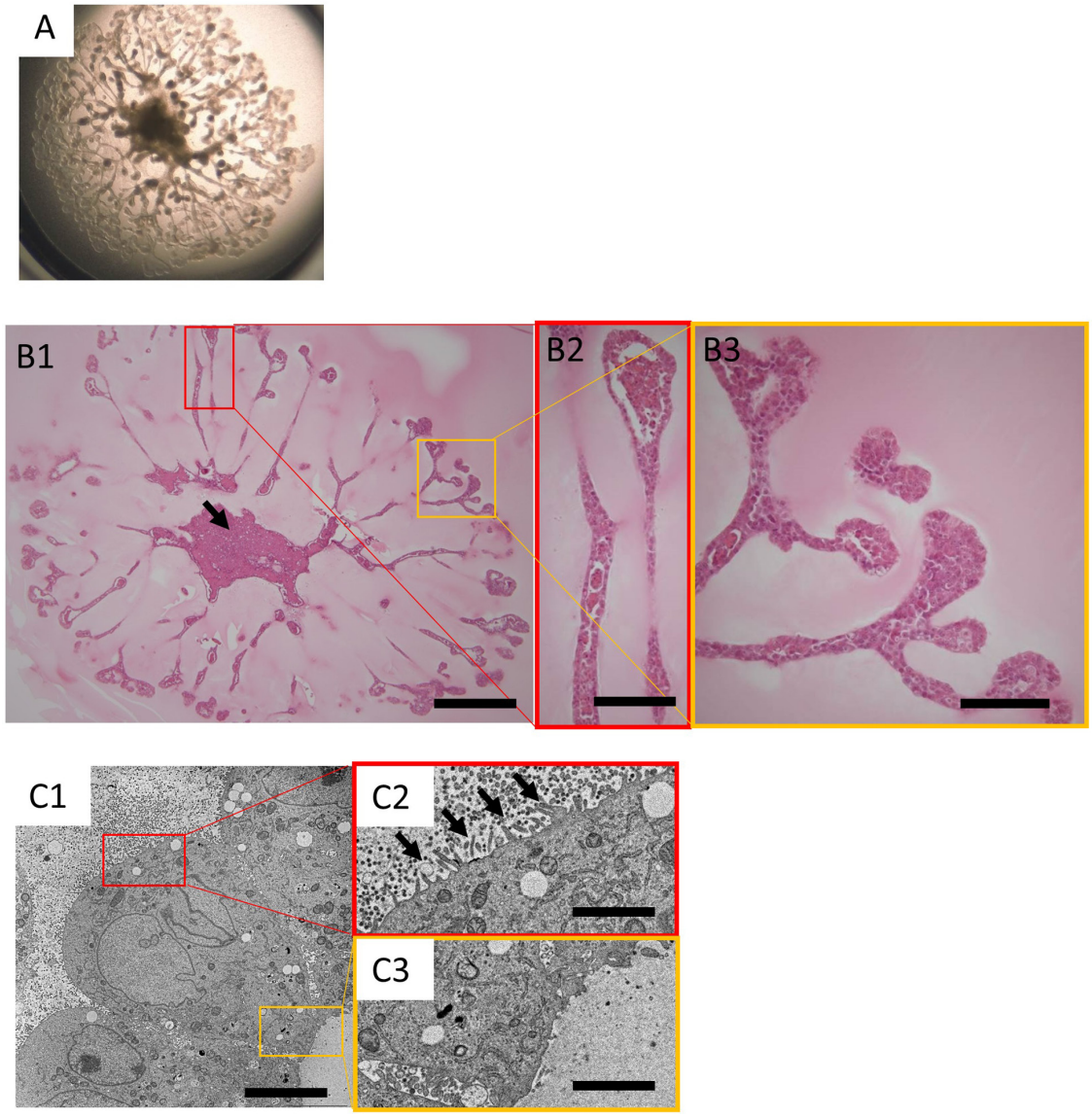


**Fig. 1.** Histology of the organoids derived from the KS cells.
A: Stereomicroscopic image of organoids derived from KS cells on day 20 in the 24-well transwell insert. B1: Histology of organoids from KS cells on day 20. The cells were mostly necrotic at the center of the culture (arrow). Haematoxylin and eosin (HE) stained; bar=600 µm. B2, B3: Magnified images of B1. The tubular structures of the organoids were generally lined with a single layer of cells. The tip of the tubular structure was bulged, and small cell populations were often trapped within the tubular structure. HE stained sections; bar=150 µm. C1: Electron microscopic image of organoids derived from KS cells on day 20; bar=5.0 µm. Magnified images of the luminal side (C2) and outer side (C3) of the tubular structure; bar=1.25 µm.

mately one layer of aligned cells, with almost no gaps. The tip of the tubular structure was bulged in comparison to the tubular extension itself. Occasionally, small cell populations were trapped within the tubular structures. At the center of the culture, the cells were mostly necrotic, except for the surface layer (Fig. 1B1, arrow).

In the images of the tubular structure obtained using electron microscopy (Fig. 1C), short villi were observed on the luminal side (Fig. 1C2, arrows). Contrarily, villi were not observed on the outer side (Fig. 1C3). In general, intercellular adhesion was loose and villi were observed in the gaps.

### *Renal proximal tubule-related markers expressed by the organoids derived from the KS cells*

Immunohistochemistry results showed that Aqp1 (a marker of the renal proximal tubule) was localized in the luminal wall of the tubular structures (Fig. 2A). The observed Aqp1 localization was consistent with its expression in the renal proximal tubule within the living body.

Meanwhile, qPCR gene expression analysis indicated that Aqp1 expression was significantly higher in the whole organoids (3D culture) than in the 2D culture of parental KS cells (Fig. 2B1). In addition, Mate1 (*Slc47a1*) expression, a

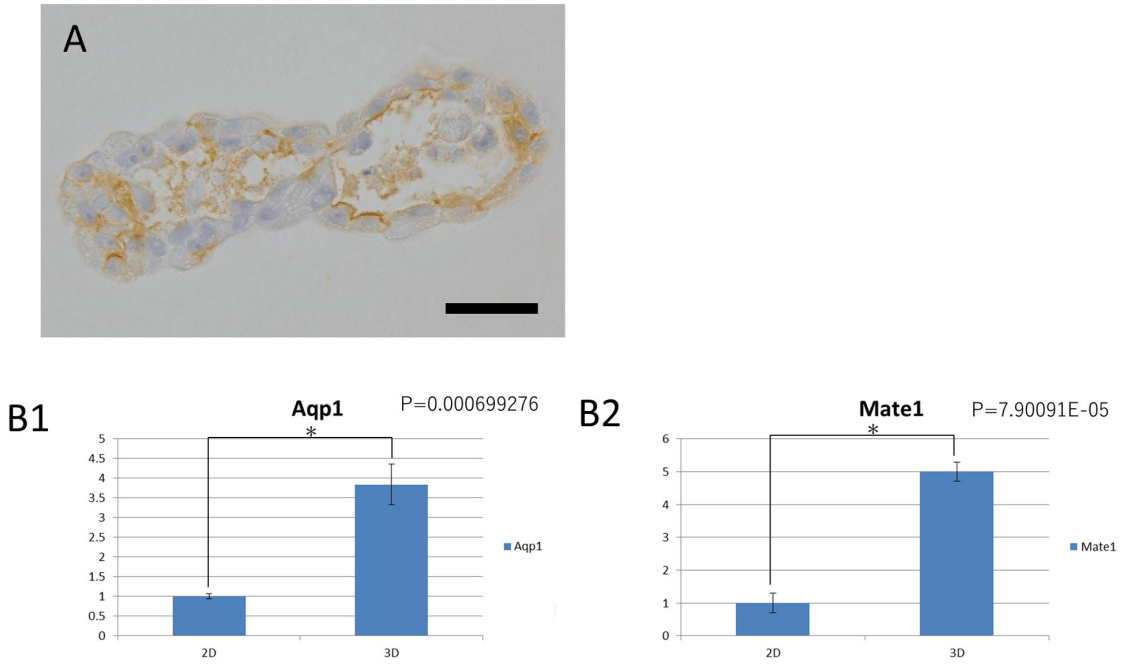


**Fig. 2.** Renal proximal tubule-related markers expressed by the organoids derived from KS cells.
A: Immunohistochemical staining of the proximal renal tubular marker Aqp1. The positive sites correspond to the lumen of the tubular structure; bar=30 μm. B: Relative comparison of the gene expression levels of Aqp1(B1) and Mate1(B2) in 2D and 3D cultures. In 2D culture, KS cells on a 10 cm plate dish at approximately 70% confluency were collected. In the 3D culture, 10 organoids cultured for 14 days were mixed to form a single sample. The gene expression levels of Aqp1 and Mate1 was higher in the 3D cultures than in the 2D cultures.

transporter involved in the extracellular excretion of cisplatin on the apical side, was significantly more expressed in the 3D organoids compared to the 2D culture (Fig. 2B2). However, OCT1 (*Slc22a1*) and OCT2 (*Slc22a2*), two transporters involved in the intracellular uptake of cisplatin from the outer surface, and megalin, a proximal tubule marker, were not expressed by either culture methods (data not shown). Thus, from the viewpoint of morphology, immunohistochemistry, and gene expression, organoids extending tubular structures were similar to renal proximal tubules in the living body, albeit with some differences, such as the lack of OCT1, OCT2, and megalin genes expression.

### *Histology of cisplatin exposed organoids derived from KS cells*

Typical images demonstrating the tubular structure of the organoids exposed to cisplatin under various conditions are shown in Fig. 3. Stereomicroscopic images of the organoids after 144 h of exposure to cisplatin at 10 μM are shown in Fig. 3A, and HE-stained images of the organoids are shown in Fig. 3B (Fig. 3B2 is the magnified image of Fig. 3B1). After the exposure of the organoids to cisplatin, the cells lining the tubular structure appeared partly vacuolized (Fig. 3B2 arrowheads). In addition, the tubular structure appeared thickened, and remnants of dead cells were clearly observed within the tubule (Fig. 3B2, arrows). These findings were not observed in organoids that were not exposed to cisplatin (Fig. 3C). Regarding the electron microscopy observations, low electron density vesicles containing the remains of organelles were observed in the cytoplasm of cells exposed to cisplatin (Fig. 3D1). These findings were not often observed in organoids that were not exposed to cisplatin (Fig. 3D2). While these organelles have not been accurately identified, they resembled autophagosomes (based on their characteristic morphological features—including the presence of the remnants).

Histological comparisons were conducted between organoids exposed to different concentrations of cisplatin (0, 20, or 30 μM) and for different exposure periods (24, 48, or 144 h). The results showed that the degree of cytotoxicity increased as the exposure dose and/or exposure period increased. (Fig. 3E, Fig. 3F).

### *Immunohistochemistry evaluation of the toxic effects of cisplatin on organoids derived from KS cells*

Immunohistochemical analyses using multiple markers were performed to investigate the response of these cells to cisplatin treatment. Immunopositive cells were observed in the groups exposed to cisplatin using antibodies against γ-H2AX, a marker of DNA damage (Fig. 4A). Some of the immuno-positive staining observed were punctate (Fig. 4A3, arrowheads), while others generally involved the staining of the whole nuclei (Fig. 4A2, arrows). Immunohistochemical analysis of phospho-histone H3, a cell division marker, revealed fewer immunopositive cells in the organoids exposed to cisplatin than in the control (Fig. 4B, Fig. 4C). Finally,

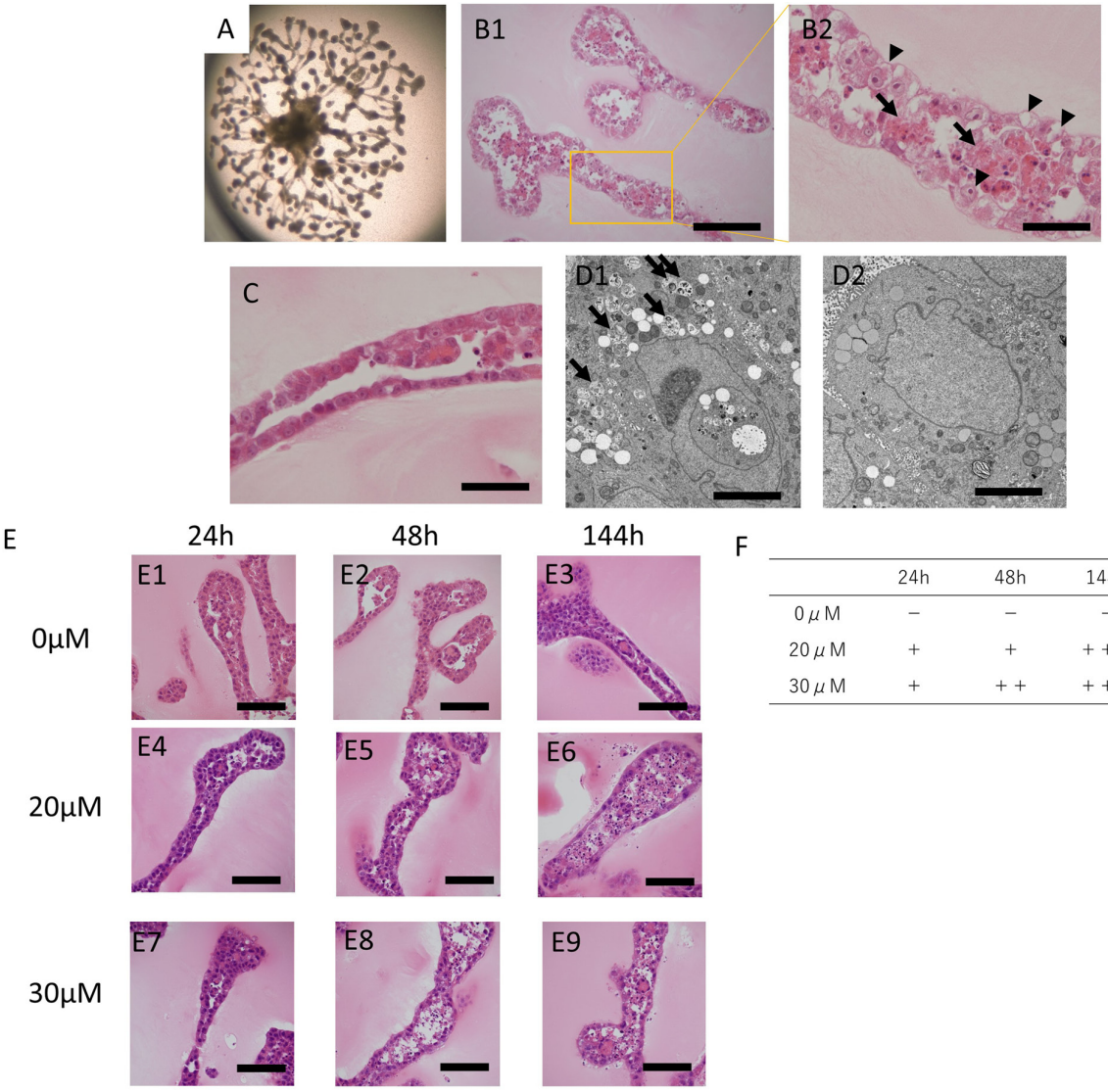


F

| | 24h | 48h | 144h |
|---|---|---|---|
| 0 μ M | − | − | − |
| 20 μ M | + | + | + + + |
| 30 μ M | + | + + | + + + |

**Fig. 3.** Histology of the cisplatin-exposed organoid derived from KS cells.
A: Stereomicroscopic image of cisplatin-exposed organoids derived from KS cells on day 20. The organoids were exposed to 10 μM cisplatin for 144 h. B1: Histology of the tubular structures of the organoids exposed to 10 μM cisplatin for 144 h. HE stained sections; bar=150 μm. B2: Magnified image of B1. Cell death was significant inside the tubular structure (arrows). Cytoplasmic vacuolization was often observed in cells constituting the tubular structure (arrowheads); bar=50 μm. C: Histology of organoids not exposed to cisplatin on day 20. HE-stained; bar=50 μm. D1: Electron microscopy image of organoids derived from KS cells exposed to 10 μM cisplatin for 144 h. Vesicles of low density containing the remains of organelles were often observed (arrows); Bar=5.0 μm. D2: Electron microscopic image of organoids, not exposed to cisplatin at day 20; Bar=5.0 μm. E: Histology of tubular structures of organoids exposed to cisplatin under various conditions. HE-stained; bar=80 μm. Organoids not exposed to cisplatin on days 15 (E1), 16 (E2), and 20 (E3). The organoids were exposed to 20 μM cisplatin for 24 h (E4; from days 14 to 15), 48 h (E5; from days 14 to 16), and 144 h (E6; from days 14 to 20). The organoids were exposed to 30 μM cisplatin for 24 h (E7; from days 14 to 15), 48 h (E8; from days 14 to 16), and 144 h (E9; from days 14 to 20). F: Scoring the cytotoxicity of the organoids under various cisplatin exposure conditions using HE sections. − = No dead cells are present in the tubular structure; + = less than 10% of all the cells in the tubules were dead; ++ = 10 to 50% of all the cells in the tubular structure were dead. +++ = >50% of all the cells in the tubular structure were dead.

immunohistochemistry using antibodies against Ki-67, a marker of cell proliferation, detected Ki-67-positive atypical cells with distorted and fairly large nuclei in organoids exposed to cisplatin for 144 h; such cells were not found in the control organoids (Fig. 4D). Comparison between Ki-67 positive cell proportions in cisplatin-exposed organoids (20 μM, 144 h) and controls showed no significant difference, although there was a decreasing trend in positive cell proportions in the cisplatin-exposed organoids (Fig. 4E).

*Cisplatin-induced apoptotic findings in organoids derived from KS cells*

To investigate apoptosis in the organoids, immunohistochemistry of cleaved caspase 3 and a TUNEL assay were performed in organoids exposed to cisplatin (Fig. 5A, Fig. 5B). After performing immunohistochemistry analysis using antibodies against cleaved caspase 3, immunopositive cells were observed in cell populations trapped inside the tubular structure and, to a lesser extent, in cells lining the tubular structure (Fig. 5A2). In the TUNEL assay, cell residues inside the tubular structure were partially positive in the cisplatin-exposed cells (Fig. 5B2).

## Discussion

In this study, we characterized kidney organoids derived from a cell line isolated from the S3 segment of rat renal proximal tubules using histopathological observations and qPCR analysis of renal tubular markers. Our results showed histopathological changes when cisplatin, a typical drug that injures the proximal tubules, was added to the organoids.

As previously reported by Kitamura *et al*.[9], these organoids contained tubular structures, and one layer of cells was consistently observed to line the tubules. Aqp1 expression was confirmed on the inner surface of the tubular structures. Moreover, the gene expression levels of renal tubular markers (such as Aqp1 and Mate1) increased after switching from the 2D to the 3D cultures. Expression of some genes related to renal proximal tubules, such as OCT1 (*Slc22a1*), OCT2 (*Slc22a2*), and megalin, was not detected in the organoids. Megalin is known to be expressed at low levels in immature proximal tubules[18]. In the organoids used in this study, immunostaining for Ki-67 (a marker of cell proliferation) and phospho-histone H3 (a marker of cell division) indicated that the cells had some proliferative capacity, suggesting that these cells were probably not fully matured; thus, some of the renal proximal tubular markers were undetected. The polarity of the microvilli in the cells was also displayed using electron microscopy. Although the organoids differed from the proximal tubules in living organisms in some aspects, they had undergone cell differentiation and were useful for toxicity assessment not mediated by OCT or megalin.

To the best of our knowledge, there have been no previous histopathological evaluations of cisplatin toxicity using renal organoids derived from rats. Toxicity studies of cisplatin using human renal organoids have been reported by Takasato *et al*. and Morizane *et al*.[19, 20] who exposed the organoids to cisplatin for 24 h; however, the present study involved long-term exposures for up to 144 h to doses of cisplatin similar to doses used in their studies. Takasato used cleaved-caspase 3 and Morizane used γ-H2AX and Kim-1 (kidney injury molecule 1: a marker of kidney injury) as indices to detect the toxicity of cisplatin. In the present study, we first compared the morphology of the cells using HE staining and electron microscopy, and then performed immunostaining using not only cleaved caspase-3 and γ-H2AX, but also phospho-histone H3 and Ki-67 (as markers), and the TUNEL method to detect toxicity. This study provides a comprehensive collection of histopathological evidence of cisplatin-induced cytotoxicity.

The toxic effects of cisplatin on organoids were both dose- and time-dependent, as confirmed by the scores of the degree of cell injury. As OCT expression was not detected, cisplatin might have permeated the cells by passive diffusion, resulting in cellular injury[21]. DNA damage, cell proliferation with distorted nuclei, and apoptosis were observed under immunohistochemistry. Immunopositive staining for the DNA damage marker γ-H2AX was observed consistently following cisplatin treatment. Some of the immunopositive stainings of γ-H2AX were punctate, but the other stainings were often widely distributed throughout the nucleus (were not punctate). Various distribution patterns of γ-H2AX have been reported by Bonner *et al*[22]. The typical distribution of γ-H2AX in DNA damage is punctate. However, pan-nuclear positivity for γ-H2AX was often observed in the apoptotic cells. These findings suggest that γ-H2AX positivity in cisplatin-exposed organoids may be the result of both DNA damage and apoptosis. Atypical cells with significantly distorted nuclei positive for Ki-67 (a marker of cell proliferation) and phospho-histone H3 (a marker of cell division) were observed in the cisplatin-exposed organoids. Bunel *et al*. reported that G2/M phase arrest occurred as a result of DNA damage caused by cisplatin, while the proportion of G2/M phase cells increased[23]. This finding suggests that exposure to cisplatin causes G2/M phase arrest in these organoids, and cells with atypical nuclei can be recognized prominently. In the semi-quantitative evaluation of phospho-histone H3, the number of immunopositive cells for phospho-histone H3 was lower in the cisplatin-exposed organoids, suggesting that cisplatin suppressed cell division. However, semi-quantitative analysis of the Ki-67-positive cells showed no significant difference between organoids treated with cisplatin and controls, although there was a decreasing trend of the rate of positive cells in the cisplatin-treated organoids. Since these two markers are found in proliferating cells, the evidence is not strong enough to conclude that cisplatin reduces the rate of cell proliferation. TUNEL test and immunohistochemical analysis of cleaved caspase 3 (markers of apoptosis) revealed that immunopositive sites were mainly located at the interior of the tubular structure of cisplatin-exposed organoids. This positive immunostaining was extensively associated with the remnants of dead cells trapped inside the tubule, suggesting that these cells underwent apoptosis. According to Anada *et al*., cell death at the center of organoids occurs due to an insufficient oxygen supply[24]. In concordance with this finding, significant cell death was observed in the central segment of the organoids in the absence of cisplatin (Fig. 1B1, arrow). It is possible that oxygen and nutrients may not be sufficiently accessible to the inside of the single-cell lining. Similarly, oxygen and medium ingredients may be lacking in the cells inside the tubular structure, compromising the viability of

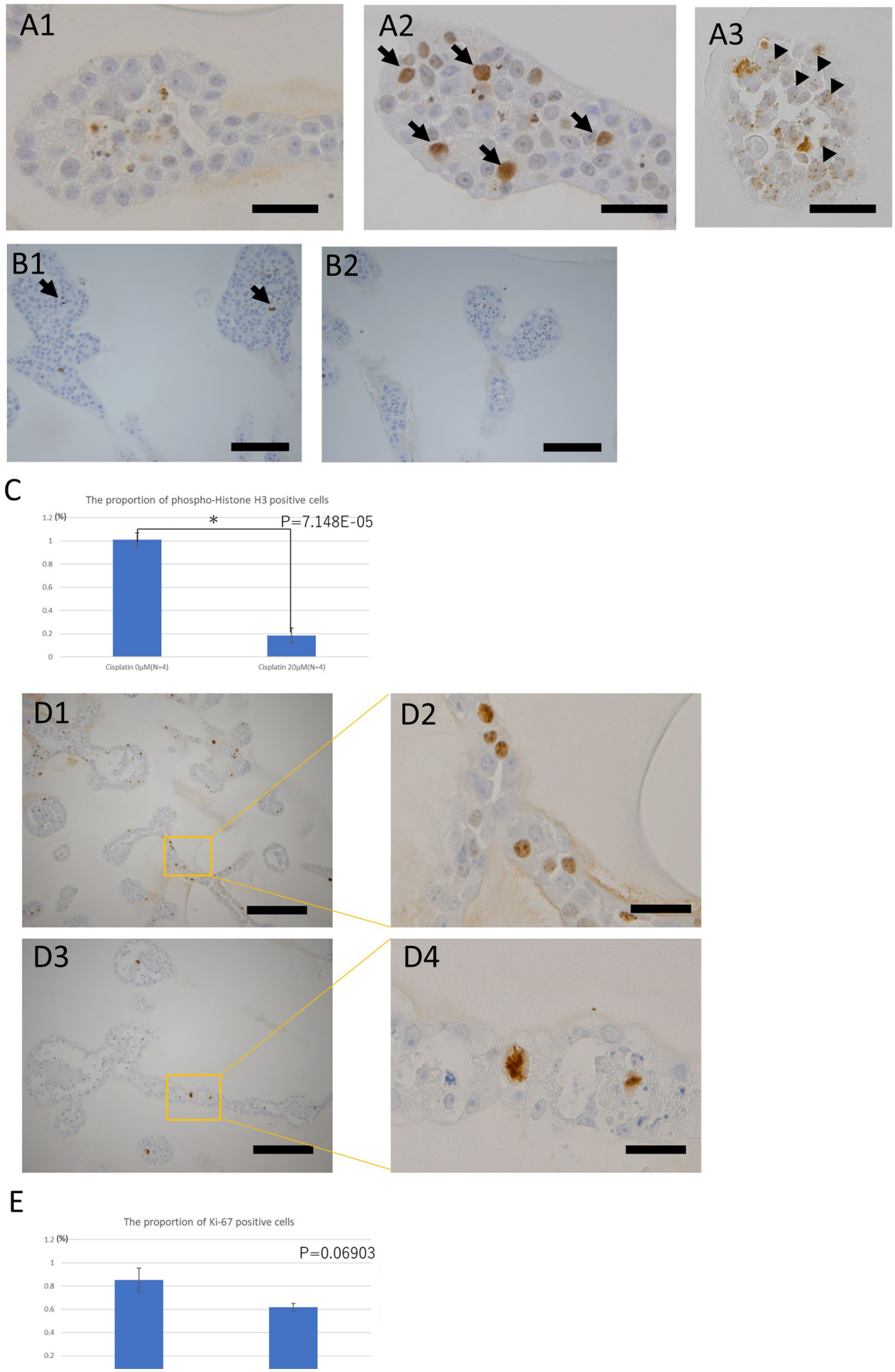
A1
A2
A3
B1
B2
C
The proportion of phospho-Histone H3 positive cells
1.2 (%)
1
0.8
0.6
0.4
0.2
0
*
P=7.148E-05
Cisplatin 0μM(N=4)
Cisplatin 20μM(N=4)
D1
D2
D3
D4
E
The proportion of Ki-67 positive cells
1.2 (%)
1
0.8
0.6
0.4
0.2
P=0.06903

**Fig. 4.**

**Fig. 4.** Immunohistochemistry studies of the toxic effects of cisplatin on the organoids derived from KS cells.
A: Immunohistochemistry of the DNA damage marker γ-H2AX. Distribution of the sites positive for γ-H2AX under each condition: bar=40 μm. A1: The nuclei of the tubular structures of the organoids not exposed to cisplatin were negative to γ-H2AX. A2: Tubular structure of organoids exposed to 30 μM cisplatin for 24 h. Positive sites for γ-H2AX often had a pan-nuclear distribution (arrows). A3: Tubular structure of organoids exposed to 10 μM cisplatin for 144 h. The positive sites for γ-H2AX had a punctate distribution in the nucleus (arrowheads). B: Immunohistochemistry of the cell division marker, phospho-histone H3. Comparison of the proportions of positive cells for each condition: bar=100 μm. B1: Tubular structures of the organoids not exposed to cisplatin. A few positive cells (dividing cells) (arrows) were observed. B2: Tubular structures of organoids exposed to 30 μM cisplatin for 144 h. No positive cells were observed. C: The proportion of phospho-histone H3-positive cells in organoids exposed or not exposed to 20 μM cisplatin for 144 h. (n=4 for both). Three tissue sections of each organoid at different levels were prepared and five randomly selected fields including the tubular structure were taken in each section. D: Immunohistochemistry of cell proliferation marker Ki-67. Comparison of morphology of positive cell nuclei under each condition. D1: Tubular structures of the organoid not exposed to cisplatin; Bar=200 μm. D2: Magnified image of D1; Bar=40 μm. D3: Tubular structures of the organoid exposed to 10 μM cisplatin for 144 h; Bar=200 μm. D4: Magnified image of D3; Bar= 40 μm. Morphologically abnormal nuclear division was observed in the organoids exposed to cisplatin. E: The proportion of Ki-67-positive cells in organoids exposed, or not exposed, to 20 μM cisplatin for 144 h (n=4 in both groups). Three tissue sections of each organoid at different levels were prepared and five randomly selected fields, including the tubular structure, were taken from each section.

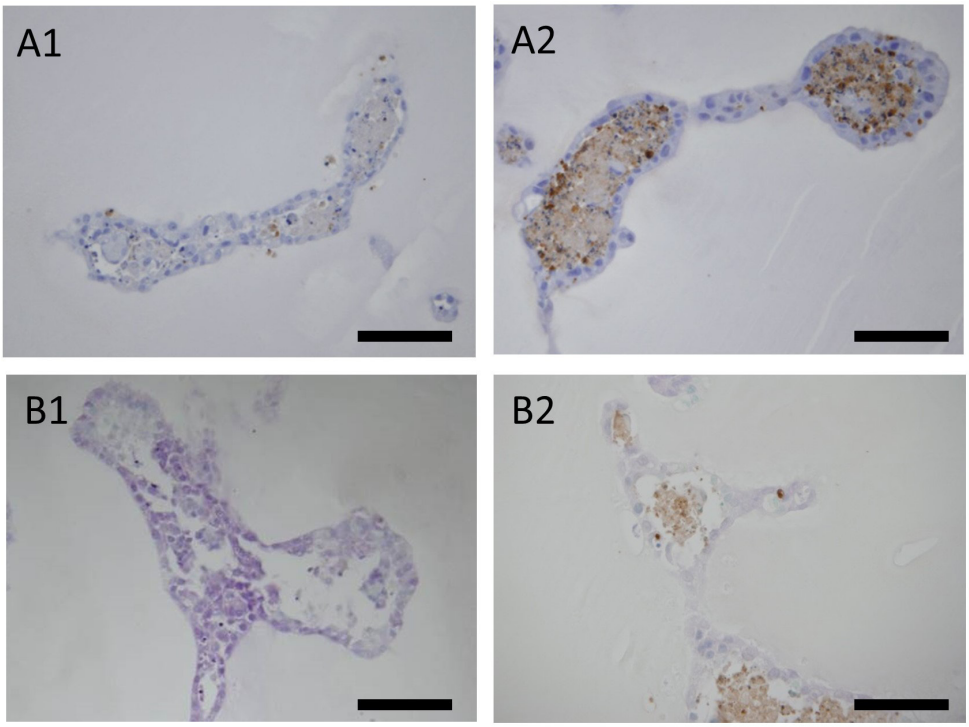


**Fig. 5.** Cisplatin-induced apoptosis in organoids derived from KS cells.
A: Immunohistochemistry of cleaved caspase 3 (apoptosis marker); bar=100 μm. A1: Tubular structures of organoids not exposed to cisplatin. A2: Tubular structures of organoids exposed to 20 μM cisplatin for 144 h. Positive sites were often observed inside the tubular structure. B: TUNEL assay of organoids derived from KS cells (bar=100 μm). B1: Tubular structures of organoids not exposed to cisplatin. B2: Tubular structures of the organoids exposed to 10 μM cisplatin for 144 h. Positive sites were observed mainly inside the tubular structures.

these cells. Consequently, the susceptibility of cells inside the tubule to cisplatin may be higher than that of the healthy surface cells.

In this study, we detected the toxicity effects (such as abnormal cell morphology, DNA damage, apoptosis, and proliferative cell abnormalities) of cisplatin at the cellular level by using conventional histopathology. These toxicological findings suggest that this culture system could serve as a model to evaluate the toxicity of cisplatin on the renal proximal tubules of rats. However, many challenges remain, ranging from the quantitative evaluation of the toxicity to the extrapolation of the results to living organs. Thus, the utility of these organoids as toxicity prediction models warrants further investigation. Toxic substances other than cisplatin should be evaluated using this system. Worth noting, this kidney organoid does not fully mimic the proximal tubule, as indicated by the lack of expression of some renal markers. Therefore, we must first confirm whether the test substance

passes through the transporters or is expressed in the organoids. Nonetheless, important toxicological findings can be obtained by using this *in vitro* system. Our results show that this kidney organoid is a useful system for the assessment of nephrotoxicity, and its histological evaluation will help to fully elucidate the mechanisms underlying nephrotoxicity. This *in vitro* system can also be incorporated as a screening tool during drug development. This study contributes to the development of alternative methods to animal experimentations.

**Disclosure of Potential Conflicts of Interest:** The authors declare that they have no competing interests.

**Acknowledgments:** We would like to thank Dr. Kumiko Ogawa of the National Institute of Health Sciences for providing comprehensive advice, Mr. Shoji Yashima of Tottori University for assisting with the histopathological procedures, and Mr. Takashi Horie of Tottori University for assistance with the electron microscopy procedures.

## References

1. Eiraku M, Watanabe K, Matsuo-Takasaki M, Kawada M, Yonemura S, Matsumura M, Wataya T, Nishiyama A, Muguruma K, and Sasai Y. Self-organized formation of polarized cortical tissues from ESCs and its active manipulation by extrinsic signals. Cell Stem Cell. **3**: 519–532. 2008. [Medline] [CrossRef]
2. Sato T, Vries RG, Snippert HJ, van de Wetering M, Barker N, Stange DE, van Es JH, Abo A, Kujala P, Peters PJ, and Clevers H. Single Lgr5 stem cells build crypt-villus structures in vitro without a mesenchymal niche. Nature. **459**: 262–265. 2009. [Medline] [CrossRef]
3. Willyard C. The boom in mini stomachs, brains, breasts, kidneys and more. Nature. **523**: 520–522. 2015. [Medline] [CrossRef]
4. Fujii E, Yamazaki M, Kawai S, Ohtani Y, Watanabe T, Kato A, and Suzuki M. A simple method for histopathological evaluation of organoids. J Toxicol Pathol. **31**: 81–85. 2018. [Medline] [CrossRef]
5. Lancaster MA, and Knoblich JA. Organogenesis in a dish: modeling development and disease using organoid technologies. Science. **345**: 1247125. 2014. [Medline] [CrossRef]
6. Rossi G, Manfrin A, and Lutolf MP. Progress and potential in organoid research. Nat Rev Genet. **19**: 671–687. 2018. [Medline] [CrossRef]
7. Takebe T, Sekine K, Enomura M, Koike H, Kimura M, Ogaeri T, Zhang RR, Ueno Y, Zheng YW, Koike N, Aoyama S, Adachi Y, and Taniguchi H. Vascularized and functional human liver from an iPSC-derived organ bud transplant. Nature. **499**: 481–484. 2013. [Medline] [CrossRef]
8. Kriks S, Shim JW, Piao J, Ganat YM, Wakeman DR, Xie Z, Carrillo-Reid L, Auyeung G, Antonacci C, Buch A, Yang L, Beal MF, Surmeier DJ, Kordower JH, Tabar V, and Studer L. Dopamine neurons derived from human ES cells efficiently engraft in animal models of Parkinson's disease. Nature. **480**: 547–551. 2011. [Medline] [CrossRef]
9. Kitamura S, Sakurai H, and Makino H. Single adult kidney stem/progenitor cells reconstitute three-dimensional nephron structures in vitro. Stem Cells. **33**: 774–784. 2015. [Medline] [CrossRef]
10. Kitamura S, Yamasaki Y, Kinomura M, Sugaya T, Sugiyama H, Maeshima Y, and Makino H. Establishment and characterization of renal progenitor like cells from S3 segment of nephron in rat adult kidney. FASEB J. **19**: 1789–1797. 2005. [Medline] [CrossRef]
11. Furukawa S, Nagaike M, and Ozaki K. Databases for technical aspects of immunohistochemistry. J Toxicol Pathol. **30**: 79–107. 2017. [Medline] [CrossRef]
12. Cerretelli G, Zhou Y, Müller MF, Adams DJ, and Arends MJ. Ethanol-induced formation of colorectal tumours and precursors in a mouse model of Lynch syndrome. J Pathol. **255**: 464–474. 2021. [Medline] [CrossRef]
13. Alam MW, Borenäs M, Lind DE, Cervantes-Madrid D, Umapathy G, Palmer RH, and Hallberg B. Alectinib, an anaplastic lymphoma kinase inhibitor, abolishes ALK activity and growth in ALK-positive neuroblastoma cells. Front Oncol. **9**: 579. 2019. [Medline] [CrossRef]
14. Moroki T, Matsuo S, Hatakeyama H, Hayashi S, Matsumoto I, Suzuki S, Kotera T, Kumagai K, and Ozaki K. Databases for technical aspects of immunohistochemistry: 2021 update. J Toxicol Pathol. **34**: 161–180. 2021. [Medline] [CrossRef]
15. Zhang G, Zeng X, Han L, Wei JA, and Huang H. Diuretic activity and kidney medulla AQP1, AQP2, AQP3, V2R expression of the aqueous extract of sclerotia of Polyporus umbellatus FRIES in normal rats. J Ethnopharmacol. **128**: 433–437. 2010. [Medline] [CrossRef]
16. Guo J, Wang L, Xu H, and Che X. Expression of non-neuronal cholinergic system in maxilla of rat in vivo. Biol Res. **47**: 72. 2014. [Medline] [CrossRef]
17. Julian GS, de Oliveira RW, Perry JC, Tufik S, and Chagas JR. Validation of housekeeping genes in the brains of rats submitted to chronic intermittent hypoxia, a sleep apnea model. PLoS One. **9**: e109902. 2014. [Medline] [CrossRef]
18. Hochane M, van den Berg PR, Fan X, Bérenger-Currias N, Adegeest E, Bialecka M, Nieveen M, Menschaart M, Chuva de Sousa Lopes SM, and Semrau S. Single-cell transcriptomics reveals gene expression dynamics of human fetal kidney development. PLoS Biol. **17**: e3000152. 2019. [Medline] [CrossRef]
19. Takasato M, Er PX, Chiu HS, Maier B, Baillie GJ, Ferguson C, Parton RG, Wolvetang EJ, Roost MS, Chuva de Sousa Lopes SM, and Little MH. Kidney organoids from human iPS cells contain multiple lineages and model human nephrogenesis. Nature. **526**: 564–568. 2015. [Medline] [CrossRef]
20. Morizane R, Lam AQ, Freedman BS, Kishi S, Valerius MT, and Bonventre JV. Nephron organoids derived from human pluripotent stem cells model kidney development and injury. Nat Biotechnol. **33**: 1193–1200. 2015. [Medline] [CrossRef]
21. Eljack ND, Ma HYM, Drucker J, Shen C, Hambley TW, New EJ, Friedrich T, and Clarke RJ. Mechanisms of cell uptake and toxicity of the anticancer drug cisplatin. Metallomics. **6**: 2126–2133. 2014. [Medline] [CrossRef]
22. Bonner WM, Redon CE, Dickey JS, Nakamura AJ, Sedelnikova OA, Solier S, and Pommier Y. GammaH2AX and cancer. Nat Rev Cancer. **8**: 957–967. 2008. [Medline] [CrossRef]

23. Bunel V, Antoine MH, Nortier J, Duez P, and Stévigny C. Potential nephroprotective effects of the Chinese herb *Angelica sinensis* against cisplatin tubulotoxicity. Pharm Biol. **53**: 985–994. 2015. [Medline] [CrossRef]

24. Anada T, Fukuda J, Sai Y, and Suzuki O. An oxygen-permeable spheroid culture system for the prevention of central hypoxia and necrosis of spheroids. Biomaterials. **33**: 8430–8441. 2012. [Medline] [CrossRef]